Research Article **Open Access**

Performance Simulation of Two-Bed Adsorption Refrigeration Chiller with Mass Recovery

Najeh Ghilen[1,2]*, Slimane Gabsi[2], Riad Benelmir[1] and Mohammed El Ganaoui[1]

[1]Faculty of Sciences and Technology, UIT Longwy Lab, University of Lorraine, France
[2]Research Unit Environment, Catalysis and Process Analysis, The National Engineering School of Gabes, Tunisia

Abstract

The technology of adsorption chiller is an efficient way of heat conversion. It can significantly reduce environmental pollution and improve energy efficiency. This paper deals with numerical study of refrigeration systems with silica gel/water pairs with mass recovery. The model is validated with experimental results from the ENERBAT platform. Numerical results are in good agreement with those of experiment. A process of mass recovery is added to study its the effect on the performances of the system. The effect of hot water temperature, cooling water temperature, chilled water temperature and cycle time, on the coefficient of performance (COP), the specific cooling capacity (SCP), the cycled mass, the evaporator outlet temperature and efficiency system are investigated in order to extrapolate the results in the Tunisian climate and to determine their optimum values able to maximize the performance of the system under analysis. The simulation calculation indicates a COP value of 0.7 with a driving source temperature of 85°C in combination with coolant inlet and chilled water inlet temperature of 40°C and 15°C, respectively. The most optimum adsorption-desorption cycle time is approximately 1240s based on the performance from COP and SCP, achieving a SCP of 400 W/kg.

Keywords: Solar adsorption refrigeration; Silica gel; Simulation; Performance; Mass recovery

Abbreviations: A: Heat transfer area (m^2); Cp: Specific heat (kJ/kg.K); DS0: Coefficient (m^2/s); E: Heat exchanger efficiency; L: Latent heat of vaporization (kJ/kg); m: Mass (kg); ṁ$_f$: Mass flow rate (kg/s); ΔH: Isosteric heat of adsorption (kJ/kg); P: Pressure (Pa); Q: Heat (kJ); SCP: Specific Cooling Power (kW/kg); t: Time (s); T: Temperatures (°C); U: Overall conductance (W/m^2.K); w,w*: Instantaneous Uptake, Equilibrium uptake (kg de réfrigérant/kg d'adsorbant); COP: Coefficient of performance of the chiller subscripts; a: Adsorbent (silica gel); ad: Adsorber; ads: Adsorption; cd: Condenser; ev: Evaporator; de: Desorber; f: Coolant; in: Inlet; j: Coolant indice; max: Maximum; min: Minimum; num: Numerical; out: Outlet; r: Refrigerant; rv: Refrigerant vapor; ref: Cooling; rec: Recovery; v: Vapor

Introduction

With the increasing economic development and environment protection, adsorption refrigeration technology as the green refrigeration method has received much attention. Adsorption refrigeration can be driven by low-grade heat source, such as waste heat from the process industry and solar energy. Thus, the adsorption technology can enhance the energy utilization efficiency for recovering low-grade heat and reduce fossil resource consumption. Furthermore, environment friendly refrigerants are used in adsorption refrigeration, making the refrigeration system simple and adsorption chiller with low noise performance.

In this context, silica gel-water was selected as the adsorbent-adsorbate pair. Compared with other adsorbents, silica gel can be regenerated at a relatively low temperature. It also has a large uptake capacity for water which has a high latent heat of evaporation; up to 40% of its dry mass. A silica gel-water adsorption chiller is able to make use of industrial waste heat to effect useful cooling. The potential for the two-bed silica gel-water adsorption chiller was evaluated by a number of researchers [1-7]. Hence, this refrigerant couple is widely studied experimentally in the literature.

Ahmed et al. [8] investigated the effect of changing fin spacing,

generation temperature lift on chiller performance of a silica-gel/water adsorption system. Evangelos et al. [9] the effect of the heat-exchanger design parameters and the effect of space velocity of the thermofluid on system performance.

Tso et al. [10] modeled a composite adsorbent consisting of two physical adsorbents. They combined silica-gel and activated carbon and modeled its use in an adsorbent system for water chilling from 14 to 9°C. They found improved COP, 0.65 and SCP, 380 W kg^{-1}, compared with either of the pure silica-gel (0.49 COP and 245 W kg^{-1} SCP) and the pure activated carbon (0.41 for COP and 189 W kg^{-1} for SCP). Glaznev and Aristov [11] investigated the effects of adsorbent grain size on the cooling capacity of silica gel. They investigated the adsorption kinetics during very fast changes in temperature for silica gel grains of various sizes. Based on their experimental results, they predicted very high maximum cooling capacities (approaching 10 kW kg^{-1}) for grains bound directly to a metal plate in the adsorbent bed. Wang et al. [12] investigated the effect of variable temperature sources on the performance of a solar driven silica-gel/water system. They saw significant changes, between 3.7-7%, in the COP depending on how the temperature of the system and the source varied compared to the operation where the temperature was constant.

Li and Wu [13,14] investigated varying temperature sources and found that lower source temperatures during the desorption phase

decreased the cooling capacity, but occasionally yielded higher COPs, while increasing the temperature over the desorption phase led to a decrease in both cooling capacity and COP. Variations in cooling load were also considered and the average cooling load over a cycle was found to be more important for predicting system performance than the variations in the cooling load over time. A two-bed, two-condenser and two-evaporator heat and mass recovery process was explored experimentally by Chen et al. [15]. They removed the check valves usually used in a system to regulate the flow from the evaporator and condenser and instead actively controlled the valve to improve the heat and mass recovery. They noted improved system performance but did not quantify the amount of improvement.
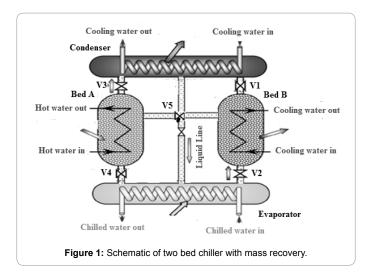
A novel three-bed, two-evaporator system was proposed and modeled by Miyazaki et al. [16]. The dual evaporator allows two beds to be adsorbing simultaneously, while a third is desorbing. A bed is connected to a low pressure evaporator and then when reaching near saturation conditions for that bed, it is connected to a high pressure evaporator and adsorption continues. COP for this system design increased by 70%, while SCC increased by 50% for this system design compared to a standard adsorption chiller working at the same conditions. Sadeghlu et al. [17], divided combined ADRS into four types based on different arrangements of two working pairs, Zeolite 13x/$CaCl_2$-water and Silica gel (RD type)-water, to analyze the performance of combined ADRS. After validating mathematical models with available experimental data, ADRS is simulated by using Simulink-Matlab software to achieve optimum times for various processes. The results of simulation show that the cooling capacity of the system with Zeolite 13x/$CaCl_2$-water is more than the other types. The results have shown that the arrangement of adsorbents affects cooling capacity of combined ADRS significantly. In Type A, Zeolite 13x/$CaCl_2$-water has been used as an adsorbent for both top and bottom cycles. This type not only has more cooling capacity than the other types, but also the effect of hot water temperature on cooling capacity of this type is less than the others. Furthermore, a sensitivity analysis has been done to determine the importance of each parameter on ADRS system because the cooling capacity and the COP are influenced by many constant parameters.

The objective of this paper is the development of a global simulation model flexible in changing operating conditions using Simulink-matlab. The optimization tools are used to enable selecting the optimum operating conditions corresponding to the best performance.

Working Principle of a Two-Bed Adsorption Chiller with Mass Recovery Scheme

The schematic diagram of the proposed two-bed mass recovery chiller is shown in Figure 1. The adsorbent bed is connected to the evaporator or condenser by flap valves operated by the effect of pressure difference between heat exchangers during adsorption or desorption respectively. On the other hand, the flow of cooling and heating water to the adsorbent bed, flow of the chilled water through the evaporator and flow of cooling water to the condenser are controlled by 5 pneumatic valves, shown in Table 1.

To operate the simulated chiller, each adsorption cycle consists of two operating modes namely; adsorption/desorption and mass recovery modes. In the adsorption/desorption mode the adsorbent bed-A is heated up by means of heating water stream (the heat source-hot water-is heated by solar radiation in a solar collector, stored in a storage tank and then transferred to the desorber by a circulating water pump), the adsorbate (water vapor) is desorbed from the adsorbent (the desorption

Figure 1: Schematic of two bed chiller with mass recovery.

Phase	1	2	3	4	5	6
V1	X	O	X	X	X	X
V2	X	X	X	X	O	X
V3	X	O	X	X	X	X
V4	X	X	X	X	O	X
V5	X	X	O	X	X	X
Bed A	H	H	-	C	C	-
Bed B	C	C	-	H	H	-
O: Opened; X: Closed; H: Heating; C: Cooling						

Table 1: Chiller cyclic operation and valving.

process) and condenses in the condenser. The liquid water enters in the evaporator at which the heat of the chilled water is adsorbed, while bed-B is cooled down by means of cooling water stream (usually from cooling tower). The adsorbent bed-B is connected to the evaporator to generate the cooling effect by means of evaporation; the water vapor is later on adsorbed by the adsorbents in the adsorber which has been cooled by cooling water. The cooling water exits from the adsorbent bed flow through the condenser tubes to condense the desorbed water vapor.

The second mode is the mass recovery mode, where the bypass valve between the adsorbent beds is opened to allow the water vapor flows from hot bed (bed-B) to cold bed (bed-A) by means of pressure swing. Because the difference of pressure between the elements of sorption, the process of adsorption/desorption continues. The adsorbate continues to evaporate of the generator and to transfer directly towards the adsorber until the balance of the pressures. The mass recovery time should be extended until the mechanical equilibrium (pressure equilibrium) between the adsorbent bed reactors, where the excess time is not recommended.

Mathematical Model

Assumptions

In order to develop a mathematical model, a number of assumptions are required.

- ✓ The temperature, pressure and the amount of water vapor adsorbed are uniform throughout the adsorber beds.

- ✓ There is no external heat loss to the environment as all the beds are well-insulated.

✓ The condensate can flow into the evaporator easily.

✓ All desorbed water vapor from the desorber will flow into the condenser immediately and the condensate will flow into the evaporator directly (no accumulation of steam in the desorber, what allows the increase of rate of desorption and condensation).

✓ The condensate will evaporate instantaneously in the evaporator and will be adsorbed in the adsorber immediately.

✓ The adsorbed phase is considered as a liquid and the adsorbate gas is assumed to be an ideal gas.

✓ The thermal resistance between the metal tube and the adsorbent bed is neglected.

✓ Flow resistance arising from the water flowing in the pipeline is neglected.

✓ The properties of the fluid, the metal tube and adsorbate vapor are constant.

According to these assumptions, the dynamic behavior of heat and mass transfer inside different components of the adsorption chiller can be written as shown below.

Rate of adsorption/desorption

The rate of adsorption or desorption is calculated by the linear driving force kinetic equation, The coefficients of LDF equation for silica gel/water are determined by Chihara and Suzuki [18] and are given in Table 2:

$$\frac{\partial w}{\partial t} = K_s \left(w^* - w \right) \text{ (kg/kg.s)} \tag{1}$$

The effective mass transfer coefficient inside the pores k_s is given by:

$$K_s = F_0 \frac{D_s}{R_p^2} \text{ (s-1)} \tag{2}$$

The effective diffusivity is defined as follows

$$D_s = D_{s0} e^{-E_a/RT} \text{ (m}^2\text{/s)} \tag{3}$$

Where,

D_{so}=2.54 10-4 m²/s, RP=1.7 10⁻⁴ m, E_a=4.2 104 J/mol, F0=15

R=8,314 J/mol K

The equilibrium uptake of silica gel-water pair is estimated using the equation developed by Boelman.

$$w^* = 0.346 \left(\frac{P_s\left(T_r\right)}{P_s\left(T_a\right)} \right)^{1/1.6} \text{ (kg}_{water}\text{/kg}_{silica\,gel}\text{)} \tag{4}$$

Where, $P_s\left(T_w\right)$ and $P_s\left(T_s\right)$ are respectively the corresponding saturated vapor pressures of the refrigerant at temperatures T_r (water vapor) and T_a (adsorbent). P_s for water vapor is estimated using the following equation:

$$P_s\left(T\right) = 133,32 \exp\left(18,3 - \frac{3820}{T - 46,1} \right) \tag{5}$$

Energy balance of adsorber

The adsorption energy balance is described by:

$$\left(m_{ad}c_{ad} + m_a c_a + m_a w c p_r + m_a w c p_{rv}\right) \frac{dT_{ad}}{dt} = m_a \Delta H_{ads} \frac{dw}{dt} + m_a c p_{r,v} \frac{dw}{dt} \left[\varphi\left(T_{ev} - T_{ad}\right) + \left(1 - \varphi\right)\left(T_{r,v} - T_{ad}\right) \right] + \dot{m}_{f,ad} c p_f \left(T_{j,in} - T_{j,out}\right) \tag{6}$$

Where, φ is either 1 or 0 depending on whether the bed is connected with evaporator or another bed. The left hand side of the adsorber energy balance equations (Equation 6) provides the amount of sensible heat required to cool the silica-gel (a), the water (r) contents in bed as well as metallic (ad) parts of the heat exchanger during adsorption. This term accounts for the output of sensible heat required by the batched-cycle operation. The first term on the right hand side of Equation 6 represents the release of adsorption heat, while the second and third terms represent for the sensible heat of the adsorbed vapor. The last term on the right hand side of Equation 6 indicates the total amount of heat released to the cooling water upon adsorption. Equation 6 does not account for external heat losses to the environment as all the beds are well insulated.

The outlet temperature of cooling water can be expressed as:

$$T_{ad,out} = T_{ad} + \left(T_{ad,in} - T_{ad}\right) \exp\left(-\frac{U_{ad}A_{ad}}{\dot{m}_{f,ad} c p_{f,ad}} \right) \tag{7}$$

Energy balance of desorber

The desorption energy balance is described by:

$$(m_{de}c_{de} + m_a c_a + m_a w c p_r)\frac{dT_{de}}{dt} = m_a \Delta H_{ads}\frac{dw}{dt} + \dot{m}_{f,de}cp_f\left(T_{f,in} - T_{f,out}\right) \tag{8}$$

The left hand side of the desorber energy balance equations (Equation 8) provides the amount of sensible heat required to heat the silica-gel (*a*), the water (*r*) contents in bed as well as metallic (*ad*) parts of the heat exchanger during desorption. This term accounts for the input of sensible heat required by the batched-cycle operation. The first term on the right hand side of Equation 8 represents the input of desorption heat. The last term on the right hand side of Equation 8 indicates the total amount of heat provided by the hot water for desorption. Equation 8 does not account for external heat losses to the environment as all the beds are well insulated.

The outlet temperature of hot water can be expressed as:

$$T_{de,out} = T_{de} + \left(T_{de,in} - T_{de}\right)\exp\left(-\frac{U_{de}A_{de}}{\dot{m}_{f,de}cp_f}\right) \tag{9}$$

Energy balance of condenser

The condenser energy balance equation can be written as:

$$(m_{r,cd}cp_r + m_{cd}c_{cd})\frac{dT_{cd}}{dt} = -m_a\frac{dw_{des}}{dt}L_v - m_a cp_{r,v}\frac{dw_{des}}{dt}\left(T_{de} - T_{cd}\right) + \dot{m}_{f,cd}cp_f\left(T_{f,in} - T_{f,out}\right) \tag{10}$$

Where the subscripts *f,cd* and *cd* indicate cooling water and condenser, respectively. The left hand side of Equation 10 represents the sensible heat required by the metallic parts of heat exchanger tubes due to the temperature variations in the condenser. On the right hand side, the first term gives the latent heat of vaporization (L_v) for the amount of refrigerant desorbed (dw_{des}/dt), the second term shows the amount of sensible heat requirement to cool down the incoming vapor from the desorber at temperature T_{de} to condenser at temperature T_{cd} and the last term represents the total amount of heat released to the cooling water.

The outlet temperature of cooling water can be expressed as:

$$T_{cd,out} = T_{cd} + \left(T_{cd,in} - T_{cd}\right)\exp\left(-\frac{U_{cd}A_{cd}}{\dot{m}_{f,cd}cp_{f,cd}}\right) \tag{11}$$

Energy balance of evaporator

The energy balance in the evaporator is expressed as:

$$(m_{ev}c_{ev} + m_{r,ev}c_{p,r})\frac{dT_{ev}}{dt} = -m_a\frac{dw_{ads}}{dt}L_v - m_a\frac{dw_{des}}{dt}c_{p,r}\left(T_{cd} - T_{ev}\right) + \dot{m}_{f,ev}c_{p,f}\left(T_{f,in} - T_{f,out}\right) \tag{12}$$

Where the subscripts *f,ev* and *ev* indicate chilled water and evaporator respectively. The left hand side of Equation 12 represents the sensible heat required by the liquid refrigerant (*r*) and the metal of heat exchanger tubes in the evaporator. On the right hand side, the first term gives the latent heat of evaporation (L_v) for the amount of refrigerant adsorbed (dw_{ads}/dt), the second term shows the sensible heat required to cool down the incoming condensate from the condensation temperature T_{cd} to evaporation temperature T_{ev} and the last term represents the total amount of heat given away by the chilled water.

The outlet temperature of chilled water can be written as:

$$T_{ev,out} = T_{ev} + \left(T_{ev,in} - T_{ev}\right)\exp\left(-\frac{U_{ev}A_{ev}}{\dot{m}_{f,ev}cp_{f,ev}}\right) \tag{13}$$

Mass balance in the evaporator

The mass balance for the refrigerant can be expressed by neglecting the gas phase as:

$$\frac{dm_{r,ev}}{dt} = -m_a\left(\frac{dw_{ads}}{dt} + \frac{dw_{des}}{dt}\right) \tag{14}$$

Where, m_a is the adsorbent mass.

System performance equations

The COP value is defined by the following equation:

$$COP = \frac{Q_{ev}}{Q_{de}} \tag{15}$$

The cooling capacity of the system is expressed by:

$$Q_{ev} = \frac{\int_0^{t_{cycle}} \dot{m}_{f,ev}cp_f\left(T_{ev,in} - T_{ev,out}\right)dt}{t_{cycle}} \tag{16}$$

Where:

Parameter	Value	Unit
m_a	50	kg
ΔH_{ads}	2800	kJ/kg
L_v	2500	kJ/kg
C_{cd}, C_{ev}, C_{ad}	0.386	kJ/kg.K
Cp_{rv}	1.85	kJ/kg.K
C_a	0.924	kJ/kg.K
C_{pr}	4.18	kJ/kg.K
$\dot{m}_{f,ad}$	1.6	m³/h
$\dot{m}_{f,cd}$	3.7	m³/h
$\dot{m}_{f,ev}$	2	m³/h
$T_{ev,in}$	15	°C
$T_{cd,in}$	22	°C
$T_{de,in}$	62	°C

Table 2: Parameters used in simulation of adsorption chiller.

$$Q_{de} = \frac{\int_0^{t_{cycle}} \dot{m}_{f,de} \, cp_f \left(T_{de,in} - T_{de,out} \right) dt}{t_{cycle}} \qquad (17)$$

Specific Cooling Power

$$SCP = \frac{Q_{ev}}{m_a} \qquad (18)$$

Results and Discussion

Model validation

Figure 2 shows the experimental and numerical inlet/outlet temperature profile of the heat transfer fluid obtained for the above mentioned standard conditions. After 7 minutes, the outlet hot water temperature is approaches her inlet temperature; at this point we have a minimum of heat consumption: the silica gel had heated thoroughly to allow desorption of water vapor. Whereas the cooling water temperature, the inlet temperature decreases during the desorption/condensation phase and increases during the preheating and precooling phase, because during the condensation /desorption process we need to extract an amount of energy to allow the condensation of desorbed water. While chilled water temperature (evaporator temperature), the outlet temperature increases during the adsorption/evaporation phase and increases during the preheating and pre-cooling phase (switching time), because during the evaporation phase, the heat to evaporate the refrigerant and cold production are needed.

The validation of the model is made for the case of a system for simple two-bed adsorption chiller, afterward the mass recovery is added to analyze the influence of mass recovery on the system performance.

Effect of hot water inlet temperature

Figure 3 presents the change in chiller cooling capacity (SCP) and COP versus hot water inlet temperature at various cooling water inlet temperatures. Other operating conditions (cycle time, chilled water inlet temperature and secondary fluid flow rate) remain constant at their design values. As the hot water inlet temperature increases the chiller cooling capacity increases for all cooling water inlet temperatures. As for COP, with hot water temperature variation from 55 to 95°C, COP increases. Because a higher hot water temperature causes a higher heating power as well as a higher refrigerating capacity. For temperatures below 85°C, remained relatively constant with the increase in the generation temperature, this is due to the insufficient refrigerant circulation required to generate the cooling power.
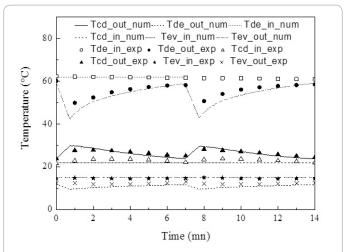

Figure 2: Overall outlet temperature profile of heat transfer fluid for two beds adsorption chiller.
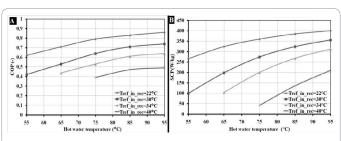

Figure 3: Generation temperature influence on chiller COP (A) and SCP (B) (Tev_in=15°C, tcycle=840 s).

It is clear that the sorption process is much faster for the highest temperatures. This means that the increase of hot water inlet temperature allows an increase in the rate of desorption and thereafter a faster heat transfer that generates the refrigerant adsorbed before the evaporation/adsorption phase.

Lowering the cooling water temperature increases the specific cooling capacity and coefficient of performance, because the condensation is faster for lower condenser cooling water temperatures, also because of the increase in adsorption rate.

The mass recovery allows the improvement of the COP and the SCP, The adsorbed and desorbed masses increase, what leads to an increase of the cycled mass and consequently an increase of the cold production.

Figure 4 shows the change in the outlet chilled temperature versus hot water inlet temperature for variable cooling water inlet temperature, there is a slight variation of the evaporator outlet temperature that decreases with an increasing the heating water temperature.

The efficiency shows the ratio between the actual coefficient of performance and the Carnot cycle coefficient of performance ideal inverse (Figure 5).

The Carnot coefficient of performance is calculated by the following relation:

$$COP_{carnot} = \left[\frac{\overline{T_{ad}} - \overline{T_{de}}}{\overline{T_{de}}} \right] * \left[\frac{\overline{T_{ev}}}{\overline{T_{ad}} - \overline{T_{ev}}} \right]$$

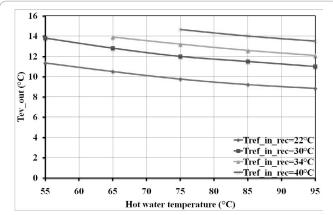The adsorption efficiency of the machine is determined by:

Figure 4: Generation temperature influence on Tev_out (Tev_in=15°C, tcycle=840 s).
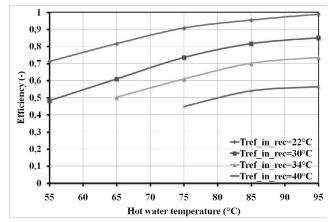

Figure 5: Generation temperature influence on chiller efficiency (Tev_in=15°C, tcycle=840 s).

$$\eta = \frac{COP}{COP_{carnot}}$$

Efficiency increases with increasing hot water inlet temperature and lowering the cooling water inlet temperature.

Effect of chilled water inlet temperature

In this part, the regeneration temperature is set at 85°C and the cooling water inlet temperature is 40°C, we will vary the chilled water temperature and see the effect on the performance of the adsorption machine.

Figure 6 shows the change in COP and SCP versus the inlet evaporator temperature, it is noted that for a variation of the latter to 20°C a variation of COP and SCP respectively 0.2 and 0.481 kW.kg⁻¹; thus increasing the evaporator inlet temperature increases evaporation rates and then increase the cold production thus increasing system performance.

Figure 7 shows the chilled water outlet temperature against its inlet temperature. It is found that the temperature difference between inlet and outlet are kept in constant, which means they are in linear relationship, for an inlet chilled water temperature of 30°C we can have a chilled outlet temperature of 26.65°C.
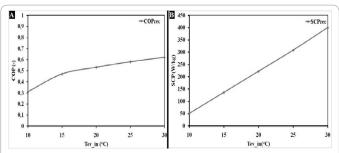

Figure 6: Effect of chilled water inlet temperature on COP (A) and SCP (B) (Tref_in=40°C, Tde_in=85°C, tcycle=840 s).
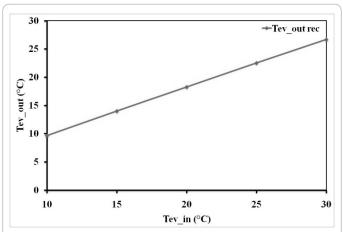

Figure 7: The relationship between chilled water outlet temperature and inlet temperature. (Tref_in=40°C, Tde_in=85°C, tcycle=840 s).

Effect of cycle time

Figure 8 shows the effect of cycle time of the adsorption/desorption process on chiller performance. The operating temperatures and flow rates are kept constant at design values, shown in Table 3.

Figure 8 shows that The COP increases uniformly with extension of the cycle time under a driving heat source of 85°C. This is because a longer cycle time causes much lower consumption of driving heat, the maximum COP can be obtained at maximum adsorption/desorption time, which correspond to the minimum heating capacity and maximum adsorbed refrigerant amount. Based on the aforementioned results, the aim is to have a short cycle time with a reasonable performance, so the optimal time 1240s cycle can be a tool to optimize adsorption system.

Conclusion

This work presents a solar adsorption refrigeration system using silica gel/water pairs. It has several advantages over the conventional system since it offers the possibility to use the free renewable energy and causes no environmental effect. We have developed a numerical model for simulating the heat and mass transfer of the adsorption and regeneration processes in the two beds with mass recovery process. This allowed us to study the influence of the regeneration, cooling, evaporator inlet temperature and cycle time on the performance of the machine. The results show that the study parameters have a great impact on system performance for its adaptation to the Tunisian climate. It is preferable to work with a high regeneration and evaporation temperature where the coefficient of performance reaches its maximum
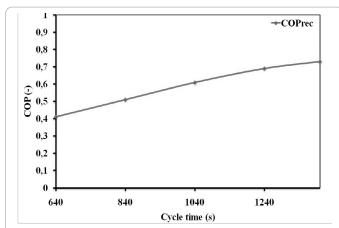
Figure 8: Effect of cycle time on the COP (Tde_in=85°C, Tref_in=40°C, Tev_in=15°C).

T_{de}_in	T_{ref}_in	T_{ev}_in	Total cycle time
85°C	40°C	15°C	640-1400 s
Pre-heating/cooling time	Hot water flow rate	Cooling water flow rate	Chilled water flow rate
40 s	1.6 m³/h	3.7 m³/h	2 m³/h

Table 3: Operating conditions.

value and a lower temperature at the cooling water of condenser and adsorber, mass recovery can improve performance. The simulation results also show that high SCP and COP of the adsorption chiller can be obtained (400 W/kg and 0.7, respectively), when the hot water temperature is 85°C, cooling water inlet temperature is 40°C and chilled water inlet temperature is 15°C.

References

1. Saha BB, Boelman EC, Kashiwagi T (1995) Computational analysis of an advanced adsorption-refrigeration cycle. Energy 20: 983-994.

2. Saha BB, Akisawa A, Kashiwagi T (2001) Solar/waste heat driven two-stage adsorption chiller: The prototype. Renew Energy 23: 93-101.

3. Saha BB, Koyama S, Kashiwagi T, Akisawa A, Ng KC, et al. (2003) Waste heat driven dual-mode, multi-stage, multi-bed regenerative adsorption system. Int J Refrig 26: 749-757.

4. Hildbrand C, Dind P, Pons M, Buchter F (2004) A new solar powered adsorption refrigerator with high performance. Solar Energy 77: 311-318.

5. Liu YL, Wang RZ, Xia ZZ (2005) Experimental performance of a silica gel-water adsorption chiller. Appl Thermal Engineer 25: 359-375.

6. Zhai XQ, Wang RZ (2010) Experimental investigation and performance analysis on a solar adsorption cooling system with/without heat storage. Appl Energy 87: 824-835.

7. Luo H, Wang R, Dai Y (2010) The effects of operation parameter on the performance of a solar-powered adsorption chiller. Appl Energy 87: 3018-3022.

8. Rezk ARM, Al-Dadah RK (2012) Physical and operating conditions effects on silica gel/water adsorption chiller performance. Appl Energy 89: 142-149.

9. Voyiatzis E, Palyvos JA, Markatos NC (2008) Heat-exchanger design and switching-frequency effects on the performance of a continuous type solar adsorption chiller. Appl Energy 85: 1237-1250.

10. Tso CY, Chao CYH, Fu SC (2012) Performance analysis of a waste heat driven activated carbon based composite adsorbent-water adsorption chiller using simulation model. Int J Heat Mass Transfer 55: 7596-7610.

11. Glaznev IS, Aristov YI (2010) The effect of cycle boundary conditions and adsorbent grain size on the water sorption dynamics in adsorption chillers. Int J Heat Mass Transfer 53: 1893-1898.

12. Wang DC, Wang YJ, Zhang JP, Tian XL, Wu JY (2008) Experimental study of adsorption chiller driven by variable heat source. Energy Convers Manage 49: 1063-1073.

13. Li S, Wu JY (2009) Theoretical research of a silica gel-water adsorption chiller in a micro combined cooling, heating and power (CCHP) system. Appl Energy 86: 958-967.

14. Wu JY, Li S (2009) Study on cyclic characteristics of silica gel-water adsorption cooling system driven by variable heat source. Energy 34: 1955-1962.

15. Chen CJ, Wang RZ, Xia ZZ, Kiplagat JK, Lu S (2010) Study on a compact silica gel-water adsorption chiller without vacuum valves: Design and experimental study. Appl Energy 87: 2673-2681.

16. Miyazaki T, Akisawa A, Saha BB (2010) The performance analysis of a novel dual evaporator type three-bed adsorption chiller. Int J Refriger 33: 276-285.

17. Sadeghlu A, Yari M, Dizaji HB (2015) Simulation study of a combined adsorption refrigeration system. Appl Thermal Engineering 87: 185-199.

18. Chihara K, Suzuki M (1983) Air drying by pressure swing adsorption. J Chem Engineering Jap 16: 293-298.